Optics Communications 341 (2015) 284–294

Contents lists available at ScienceDirect

Optics Communications

journal homepage: www.elsevier.com/locate/optcom

Spatial profile and singularities of the edge-diffracted beam with a multicharged optical vortex

A.Ya. Bekshaev *, K.A. Mohammed

I.I. Mechnikov National University, Dvorianska 2, 65082 Odessa, Ukraine

ARTICLE INFO

Article history:
Received 22 October 2014
Received in revised form
1 December 2014
Accepted 6 December 2014
Available online 12 December 2014

Keywords:
Optical vortex
Edge diffraction
Beam propagation
Spatial structure
Phase singularity

ABSTRACT

We analyze the edge diffraction of circular Laguerre–Gaussian beams LG_{02} and LG_{03} carrying multicharged optical vortices (OVs), with special attention to spatial properties and evolution of the diffracted beam. The problem is considered numerically within the frame of paraxial approximation and the Fresnel diffraction theory. The diffracted beam evolution is interpreted on the basis of the incident beam symmetry breakdown and decomposition of a higher-order OV into a set of single-charged secondary OVs. Upon propagation, the separate OVs describe specific trajectories within the diffracted beam cross section but in the far field they are localized on the symmetry axis parallel to the screen edge. The OVs' positions in each cross section reflect information of the screen edge position with respect to the incident beam axis. If the incident OV is stopped by the screen, the diffracted beam possesses no OV just behind the screen but in the course of its further propagation, single-order OVs appear consecutively so that in the far field the number of OVs equals to the absolute topological charge of the incident OV. Possible applications for the remote measurements of small linear displacements are discussed.

1. Introduction

Light beams with optical vortices (OV) [1–4] attract a steady interest due to their unique physical features. The singularity in the transverse phase profile (so called screw wavefront dislocation) with zero amplitude in the OV core is accompanied by the circulatory component of the energy flow thus forming the genuine vortex-like motion of the light energy. Such beams can spontaneously emerge during the laser generation [5] as well as be deliberately produced from the usual rectangular Hermit–Gaussian modes by means of astigmatic mode correctors [6]; the most suitable and efficient ways for their generation employ special optical elements creating the wavefront singularity: spiral phase plates [7], holographic elements with groove bifurcation ("fork") [8,9], etc. The transverse energy circulation (TEC) is coupled with corresponding mechanical properties, especially, the orbital angular momentum (OAM) of the beam with respect to the propagation axis, which is used in many applications, e.g. for micromanipulation technique [10,11]. However, more important is that the special pattern of the energy flow in OVs makes them informative and suitable physical objects for the study of deep fundamental aspects associated with the internal energy flows in light fields [12].

Among numerous physical manifestations of the specific OV peculiarities, the most immediate and physically spectacular ones are realized in the effects that accompany the OV beam propagation in presence of obstacles; even the tiny perturbations associated with the beam reflection or refraction at a smooth interface introduce the specific "topological aberrations" in the OV structure [13]. Stronger transformations of the beam configuration are coupled with the diffraction phenomena, in particular, those related to the edge [14–22], slit [17,21] and strip [22,23] diffraction. The special features of the OV beams' diffraction are employed for the OV detection and diagnostics [22–25] and even can be useful for the subwavelength optical metrology [26–29]. Together with the explicit demonstration of the circulatory flow pattern that "comes to light" due to the OV symmetry violation [12,30], the particular nature of the OV beams manifests itself in intricate behavior of the "post-diffraction" singular structure. Depending on the position and shape of an obstacle, the beam OV may "temporary" disappear but regenerate in the course of further propagation; the "survived" OVs normally displace from the nominal incident beam axis and evolve along certain trajectories; additional "secondary" OVs may appear, and the whole set of these singularities ("singular skeleton") participate in complicated topological reactions: during the diffracted beam propagation, OVs may emerge, migrate, annihilate and their morphology experiences continuous transformations [14–20,26,27,30,31].

All the above facts are important not only for actual and potential applications but also for better understanding of the

* Corresponding author.
E-mail address: bekshaev@onu.edu.ua (A.Ya. Bekshaev).

http://dx.doi.org/10.1016/j.optcom.2014.12.019
0030-4018/

peculiar properties of the OVs and associated physical phenomena. This is why the systematic investigation of the OV diffraction is a relevant and insistent task. In the recent works [31,32] we have started a comprehensive theoretical development of this problem including two complementary aspects: (i) analysis of the transverse energy redistribution over the diffracted beam on the basis of the universal approach for the TEC description which recognizes two different forms of the TEC – "vortex" and "asymmetry" TEC – that characterize, from very general positions, evolution of an arbitrary asymmetric beam profile [30,33] and (ii) direct calculation of the OV skeleton and its evolution during the diffracted beam propagation. In particular, there was demonstrated applicability of the "vortex" and "asymmetry" constituents of the beam OAM, based on the beam characterization via the space-angle irradiance moments [34–38], for characterization of the TEC in diffracted OV beams. However, the study in Refs. [31,32] was restricted to the simplest case of diffraction of a single-charged (first-order) Laguerre–Gaussian (LG) beam with radial and azimuthal indices $p=0$, $|l|=1$. This case is important since it represents a standard generic physical model of a usual OV beam but it does not include interesting situations associated with high-order OVs whose diffraction demonstrates the TEC in OV beams in the most evident and impressive way [21,22].

In this paper we represent a further development of the concepts and approaches of Refs. [31,32] in application to the diffraction of higher-order OV beams, especially with $|l|=2$ and 3. In particular, we show that diffraction of an OV beam can be interpreted in terms of the beam symmetry breakdown which is commonly known to be accompanied by decomposition of a multicharged OV into a set of $|l|$ secondary single-charged OVs. In the diffracted beam, each of these OVs evolves in its particular manner and, together with the diffraction-generated "additional" OVs, form a complicated "OV skeleton" rich in interesting and physically meaningful details.

2. Mathematical formulation

In this paper, we consider the diffraction of a paraxial monochromatic light beam with frequency ω and the wavenumber $k=\omega/c$ (c is the light velocity), for which the electric field $\mathcal{E}(t)$ is characterized by the complex amplitude E defined as $\mathcal{E}(t)=\mathrm{Re}\,[Ee^{-i\omega t}]$. Let the beam propagate along axis z; then $E\equiv E(x,y,z)=u(x,y,z)\exp(ikz)$ where (x,y) are coordinates in the transverse plane, function $u(x,y,z)$ slowly varies on the wavelength $\lambda=2\pi/k$ distance scales. Let the diffraction obstacle (screen) be situated in the transverse plane $z=0$, and the transverse coordinates in this plane be marked by the subscript a (see Fig. 1). The incident circularly symmetric OV beam is taken in the form of LG_{0m} mode [39] and in the screen plane its complex amplitude distribution obeys the equation

$$u(x_a,y_a,0)\equiv u_a(x_a,y_a)=\frac{1}{\sqrt{|m|!}}\left[x_a+i\,\mathrm{sgn}\,(m)y_a\right]^{|m|}\exp\left(-\frac{x_a^2+y_a^2}{2}\right). \quad (1)$$

In this expression, dimensionless coordinates are used so that x, y are measured in units of the Gaussian envelope radius b [31,40]; accordingly, the longitudinal coordinate is suitably measured in units of the Rayleigh range $z_R=kb^2$. For example, if the incident beam wavelength is $\lambda=632.8$ nm (He–Ne laser radiation) and the radius $b=0.1$ mm, $z_R=100$mm. Expression (1) supposes that the incident beam approaches the obstacle in its waist cross section but this implies no serious limitation since the situation of arbitrary wavefront curvature can be readily reduced to the case of plane wavefront by merely rescaling the final results [31].

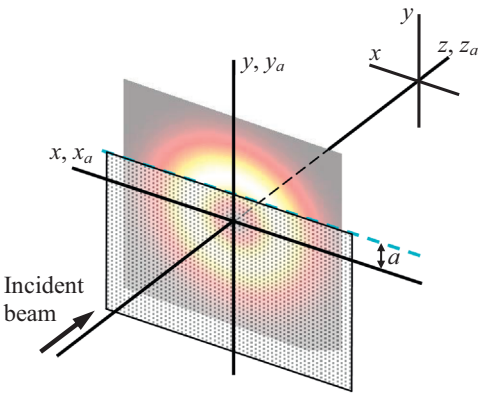

Fig. 1. Geometrical conditions of the diffraction.

Now consider diffraction of this beam at a half-plane screen in the Kirchhoff–Fresnel approximation [39,41]. If the screen edge is parallel to the x-axis and its position with respect to the incident beam axis is characterized by the dimensionless distance a (again in units of b), the beam complex amplitude in the transverse plane situated at the longitudinal distance z (in units of z_R) behind the screen (see Fig. 1) is determined by the equation of evolution (Fresnel diffraction integral) [31,41]

$$u(x,y,z)=\frac{1}{2\pi iz}\int_{-\infty}^{\infty}dx_a\int_a^{\infty}dy_a\,u_a(x_a,y_a)\exp\left\{\frac{i}{2z}\left[(x-x_a)^2+(y-y_a)^2\right]\right\}. \quad (2)$$

In case of $m=1$ in Eq. (1) this integral has a convenient analytical representation [17], which strongly facilitates the theoretical calculations [31,32]. With growing OV order, analytical representation is still available but becomes cumbersome, difficult to interpret [17,18] and does not help in calculations so the main body of this paper is devoted to the numerical investigation of Eq. (2) and its consequences.

3. Numerical examples and calculations

The evolution of the diffracted beam obtained after the edge diffraction of an LG beam (1) with $m=2$ and $m=3$ is illustrated by Figs. 2–5 calculated via Eq. (2); all the images represent the intensity or phase distribution over the beam cross section, visible against the beam propagation; the TEC in the incident beam is directed counter-clockwise. Each column of Figs. 2–5 represents evolution of the diffracted beam obtained for a fixed degree of the incident beam shading; conventionally, it is suitable to segregate the regimes of weak ($a<-0.5$, the screen only "cuts" the periphery of the beam cross section), moderate ($-0.5<a<0$, the screen strongly perturbs the beam but the axial OV is not covered) and severe ($a>0$, the incident beam OV is stopped) shading.

It is seen that just after the screen (1st–3rd rows of Figs. 2 and 3) the beam intensity pattern evolves asymmetrically: at $x<0$, the beam energy spreads into the shadow region while at $x>0$ it apparently moves "back" from the geometrical projection of the screen edge into the "bright" region so that finally main part of the beam energy is concentrated in the $x<0$ half-plane (rows 2–4 of Figs. 2 and 3). This behavior is a confirmation of the circulatory character of the transverse component of the energy flow within